Iron-based intermetallic particles formation in Al-Zn-Si alloy through powder metallurgy route

Abdul Khaliq *, I. A. Chaudhry, M. Boujelbene, Ayyaz Ahmad, I. Elbadawi

College of Engineering, University of Ha'il, Ha'il, Saudi Arabia

A B S T R A C T

Corrosion of the steel products is one of the significant challenges which is managed by coating with Al-Zn-based alloys. The Galvalume alloy (Al-55%, 43.5%-Zn, Si-1.5%) is coated on steel strips via a hot-dipping process. The dissolution of iron (Fe) from steel strips and the formation of Fe-based intermetallic particles is an inevitable phenomenon during the hot-dip coating process. These intermetallic particles are a primary source of massive bottom dross build-up in the coating pot and metal spot defects in the coated steel products. Therefore, it is important to investigate the formation of Fe-based intermetallic particles. In this study, Fe-based intermetallic particles are produced via the powder metallurgy route. High energy ball milling was used for mechanical alloying of aluminum (Al), iron (Fe), silicon (Si), and zinc (Zn) powders. Optimized ball milling conditions were identified after a series of trials. After cold pressing, the mechanically alloyed samples (pellets) were sintered at various conditions in a high vacuum sintering furnace. The X-ray diffraction (XRD) and scanning electron microscope (SEM) equipped with energy-dispersive X-ray diffraction (EDS) were used for the analysis of raw material, mechanically alloyed powders, and sintered pellets. It is concluded that the mechanical alloying of 6h and cold pressing at 9 tons for 30 min is sufficient to produce a dense compact material. It was found that Fe-based intermetallic particles were successfully fabricated which were α-AlFeSi. However, intermetallic particles similar to those found in the bottom dross of the coating pot are difficult to fabricate through the powder metallurgy route due to the volatilization of Zn during the sintering process.

1. Introduction

Steel sheets have been widely in automotive, construction, and several other engineering applications. Corrosion is a big challenge faced by steel products. Cathodic protection is one of the techniques used to protect steel against corrosion. In this process, Zn is coated which sacrificed and protect the steel products from corrosion. For better service life of steel sheets used in the building industry, Zn coatings are replaced with Al-Zn-based alloys which offer multiple benefits. Such coating alloys exhibit excellent durability of Al matrix and cathodic protection of Zn metal which significantly enhance the service life (Marder, 2000; Sheikhhasani

et al., 2016). Galvalume or Zinclume is a commercial alloy that is composed of 55% Al, 1.6% Si, and balance Zn (all compositions are given in wt.%) (Selverian et al., 1987). It has been used successfully in the industry. These alloys are coated on the steel sheets through the hot-dip coating process. In this process, a clean fast-moving steel strip is immersed into the 55%Al-Zn coating pot which is maintained at 600°C±5°C. Generally, coating pots contain 30-40 tons of molten alloy which are heated and stirred with induction heaters installed at various locations. Steel strip residence time in coating pot varies from 2-3 seconds. After passing through the coating pot, a steel sheet is introduced into a pair of air knives which remove the extra molten alloy and maintain the required coating thickness (Luo et al., 2013; Khaliq et al., 2021; 2020). The schematic diagram of the continuous hot-dip coating process can be found in Luo et al. (2013).

The hot-dip coating of the 55%Al-Zn alloy is composed of the following main features. (1) Zinc containing dendritic Al matrix which is composed of

~80% of the total coating overlay; (2) Zn rich phase which is 20% of total overlay in the interdendritic regions; (3) Intermetallic alloy layer (<2μm) between the steel substrate and coating alloy; and, (4) Mg_2Si particles in the interdendritic regions. Such framework of the coating alloy offers better corrosion properties compared to pure Zn coatings (Chen and Yuen, 2012). Therefore, steel sheets coated with 55%Al-Zn alloys are used in the construction industry for the roof panel, wall panels, insulation shell, workshop, warehouse, and barn. In the automotive industry, coated steel sheets are used for the body inside the board, water tanks, fuel tanks, exhaust pipes, silencers, fenders.

Although the continuous hot-dip galvanizing process has been used successfully in the industry the challenges of bottom dross build-up in the coating pot and metal spot defects on the cold-rolled steel sheets remain unresolved. These challenges are associated with the continuous precipitation and dissolution of Fe-based intermetallic particles in the coating pot (Peng et al., 2019). Khaliq et al. (2020) have investigated the fabrication of Fe-based intermetallic particles and their dissolution in the 55%Al-1.6%Si-Zn coating alloy. It was reported that the dissolution kinetics of Fe-based intermetallic particle (τ_{5c}) is negligible in Fe-saturated coating bath at 595°C. It was argued that the calculated mass transfer coefficient (k_m) of Fe in the unsaturated coating bath was 1.43×10^{-6} m/s which is 1000 times slower than a typical solid-liquid system. It was concluded that it is unlikely that Fe-based intermetallic particles (τ_{5c}) will re-dissolve once precipitated in the coating alloy. Such intermetallic particles are the primary source of bottom dross build-up and metal spot defects in the coated steel products.

The dross generated during the galvanized process can be classified into oxides and intermetallic types. The oxides dross includes Al and Zn oxides which are generated at the surface of the coating pot. The intermetallic dross is composed of Fe-Al, Fe-Al-Si-Zn, and Fe-Zn intermetallic particles which are precipitated in the coating pot (Masumoto, and Takebayashi, 1999). Iron-based intermetallic particles precipitate due to a change in Fe solubility in the coating pot. Temperature fluctuation is one of

the main reasons which impact Fe solubility and eventually precipitation of Fe-based intermetallic particles. The detailed mechanism has been explained in the literature (Khaliq et al., 2021). A cross-section of the bottom dross generated in the industrial 55%Al-1.6%Si-Zn coating alloy is given in the literature (Elfghi and Gunay, 2020).

The bottom dross is composed of AlFeSiZn intermetallic particles which settled at bottom of the pot with time. The density of these particles is slightly greater than the alloy which facilitates them to settle with time. These particles grow by agglomeration and their size varies from a few microns to 10 mm. The removal of the bottom dross is challenging for the galvanizing industry. The suspended dross particles are smaller in size and have the same chemical composition as of bottom dross. These particles partially leave the coating pot and become part of the coating overlay and lead to metal spot defects during cold rolling of the coated sheet products.

The role of Fe-based intermetallic particles is pivotal in determining the rate of bottom dross build-up in the coating pot and metal spot defects in the coated steel products. In this study, an effort has been made to produce Fe-based intermetallic particles via powder metallurgy route which involved mechanical alloying, pressing, and sintering steps. The fabrication of discrete Fe-based intermetallic particles will facilitate understanding the chemical and crystallography nature of the suspended and bottom dross particles. In addition to that, the dissolution kinetics of the Fe-based intermetallic particles will be possible. Therefore, this study is dedicated to the formation of Fe-based intermetallic particles via the powder metallurgy route.

2. Experimental plan and methodology

The raw material used in this study is composed of pure metal (Al, Fe, Si, and Zn) powders obtained from the Australian Metals Powders Supplies Pty Ltd. SEM images of Al, Fe, and Zn powders are shown in Fig. 1. Zinc particles are smaller and spherical compared to Al and Fe particles.
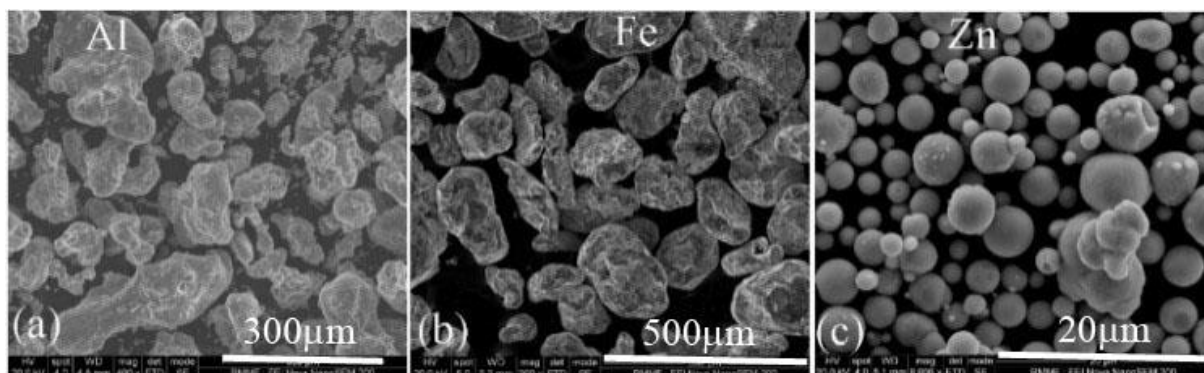

Fig. 1: SEM-SEI images of Al, Fe, and Zn metals powder

The relative weights (g) of each metal used in this study are given in Table 1.

Table 1: Weight of each element used in this study

Batch	Al	Fe	Si	Zn
1	50g	30g	6.5g	12g
2	52g	31g	6.6g	10g

In this study, a powder metallurgy route was adopted to fabricate Fe-based intermetallic particles from their metal powders. The powder metallurgy route is used for the fabrication of several products such as TiAlV and similar alloys (Elfghi and Gunay, 2020). A brief summary of mechanical alloying, cold pressing, and sintering processes are described in this section.

Mechanical alloying of the metal powders was achieved by mixing them in a QM-3SP2 planetary high-energy ball mill. During this process, metal powders are constantly pressed, coldly deformed, and fractured as a result of ball collision (Naeem et al., 2019). Cold welding and fracturing of the metal powders are commonly observed (Suryanarayana, 2001). In this study, stainless steel jars and balls with 5:1 were used. High energy ball milling was carried out at 300 rpm with 30 min milling and 15 min cooling time. The total mechanical alloying time was 6h, 12h, 18h, 24, and 30h. Stearic acid (0.5%) was used as a processing control agent (PCA) to minimize the agglomeration and sticking of the powders. The mechanically alloyed powders were studied under the scanning electron microscope (SEM) and X-ray diffraction (XRD).

After ball milling, metal powders were cold pressed into pellets using an isostatic uniaxial pressing machine. For pellets making, a 2g of mechanically alloyed powder was charged into a steel die and cold-pressed for 30 min at 6 and 9 tons. This step is critical in obtaining the dense structure in the final product. The green pellets produced are shown in Fig. 2.

Sintering is a process in which powder pellets are heated to a temperature lower than the melting point of the base elements, held for a certain time, and cooled to room temperature. During sintering, metal powder particles coalesce into a dense structure that exhibits high mechanical properties. For sintering, GSL-1600 high vacuum tube furnace was used which can reach up to 1650°C with an accuracy of ±1°C. The sintering process was carried out under oxygen partial pressure of 10-6 Pa for 24h, 48h, and 72h at 700°C.


Fig. 2: Cold pressed green pellets

After sintering, the compacts were prepared for microscopic investigation. The sintered compacts were ground using 800, 1200, and 4000 emery papers in water. The polishing was carried out at 3µm and 1µm diamond paste. The final polishing was conducted using MD-Mol, a silicon particles-based suspension. For metals powder and sintered compacts phase analysis, Philips XL30 scanning electron microscope (SEM) equipped with energy-dispersive x-ray spectroscopy was used. To determine the degree of mechanical alloying and various phases, an X-ray diffractometer (XRD, Rikagu, D/Max-rB) at a scanning rate of 1°/min over the 2θ range of 10° to 90° was used in this study.

3. Results and discussion

The mechanical alloyed and sintered AlFeSiZn samples were investigated under SEM for particle shape and morphology. Fig. 3 shows the evolution in the particles' size and shape with ball milling time. It is evident that particle sizes varied from a few microns to more than 500µm which predict cold welding of ductile particles during ball milling. Particles shape is also irregular and not showing spherical content which also supports that cold welding of the metal powder is most likely the phenomenon during ball milling.
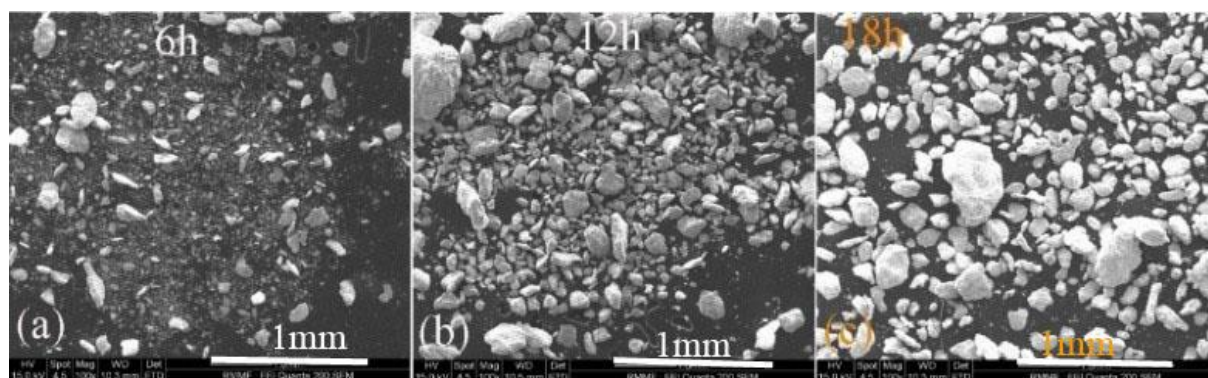

Fig. 3: SEM-SEI images of Al, Fe, Si, Zn mechanically alloyed powders. (a) 6h, (b) 12h (c) 18h

During mechanical alloying, particles diffuse into each other and make a homogenous mixture which is determined by XRD analysis. For pure metals, XRD peaks are sharp but during mechanical alloying broadening of the peaks is observed. Therefore, Fe-based intermetallic formation via mechanical alloying and subsequent sintering processes are determined by XRD analysis. Figs. 4 and 5 show the XRD plot of the mechanically alloyed samples after 6h and 24h of ball milling. It is observed that with mechanical alloying time, the % of Fe-based intermetallic (AlFeSi) has increased. The AlFeSi percentage was 38.9% after 6h of ball milling which increased to 55.5% during 24h of ball milling. It can also be observed that XRD peaks relatively broadened in 24h ball milling samples, as shown in Fig. 5. In addition to that Al peaks gradually weakened with ball milling time. The diffraction peaks of iron are gradually shifted to a large angle and appear to be broadened, which means that as the milling time is prolonged, Al and iron diffuse into each other lattice to form AlFe solid solution and eventually Fe-based intermetallic compounds (AlFeSi). AlFe intermetallic phases are commonly observed in steel alloys (Abro et al., 2020).

During mechanical alloying of 6 hours, powder particles tend to be the same in size. After continuous ball milling, most of the powder particles continue to become smaller, but some of the powder particles sizes gradually increased because of continuous cold welding, see Fig. 3b and Fig. 3c. When the particle size of the powder is increased to a certain extent due to the increase of the cold welding, the lattice distortion increases, the hardness increases, the chances of crushing are higher than cold welding, and the particle size is reduced. After 18h of ball milling, the particle size of the powder decreases gradually with the increase of milling time, but some of the powder will be agglomerated, therefore few large particles are present, Fig. 3c.
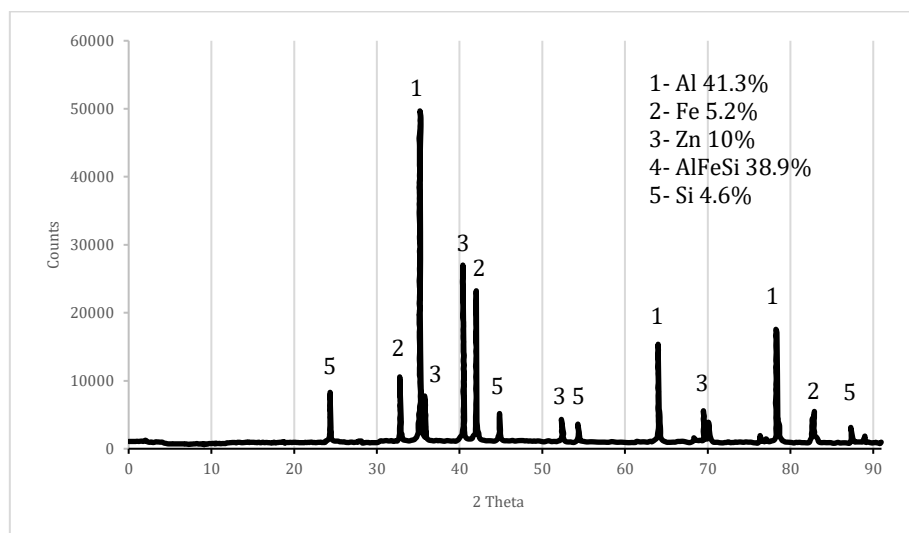
Fig. 4: XRD pattern of Al, Fe, Si, and Zn powders after 6h of ball milling time
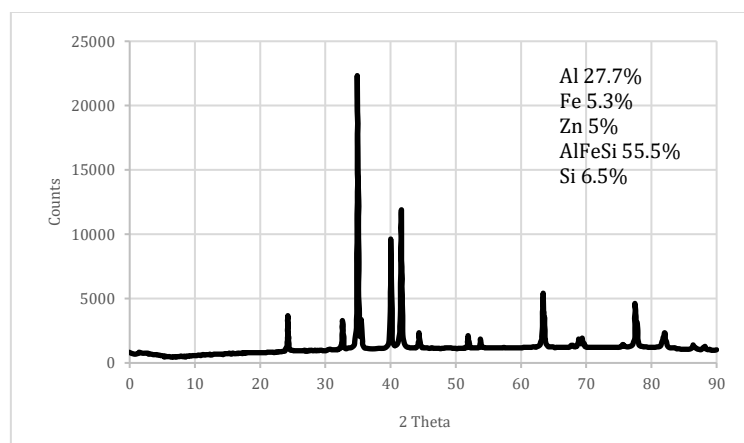
Fig. 5: XRD pattern of Al, Fe, Si, and Zn powders after 24h of ball milling time

It is summarized from the SEM and XRD analyses of the mechanically alloyed samples that cold welding is the dominant phenomenon during ball milling. With ball milling time, % of AlFeSi phase increased which reached 55.5% after 24h. These are extraordinary findings as the proportion of intermetallic phase is much higher compared to that reported in literature (Carpenter et al., 2007). The XRD plots of the samples sintering time of 24h, 48h and 72h are shown in Figs. 6-8 respectively.

The sintering temperature was 500°C considering low melting point metals (Zn, Al) in the samples.

Phase identification with certainty is not easy especially in multicomponent systems where stable and metastable phases are possible. In this system, the Fe-based intermetallic phase (AlFeSi) was 69% along with other pure metals (Al, Fe, and Si), as shown in Fig. 7. It was observed that a sintering time of 48h is sufficient to produce the maximum possible AlFeSi phase under the given conditions. Further increasing the sintering time to 48h has not yielded a better outcome. Zinc phase was not detected in all the samples after sintering at 700°C in a high

vacuum furnace. Zinc was volatilized during the sintering process due to low partial pressure. Therefore, Zn turns into vapors and later on oxidized to form ZnO, which was observed in samples after 48h of sintering, see Fig. 8.

The sintered compacts were prepared for metallographic study and analyzed under SEM equipped with an EDS detector. Fig. 9 shows SEM-SEI of the Al, Fe, Si, Zn compacts sintered at 700°C for 24h, 48h, and 72h.
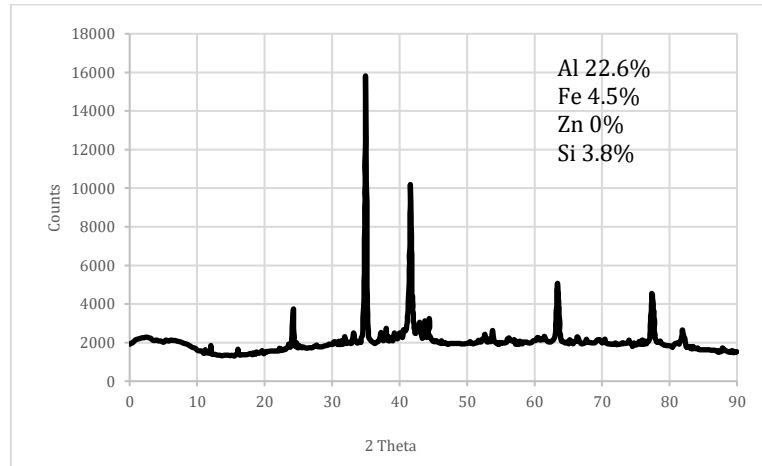
Fig. 6: XRD pattern of Al, Fe, Si, and Zn mechanical alloyed powders sintered at 700°C for 24h
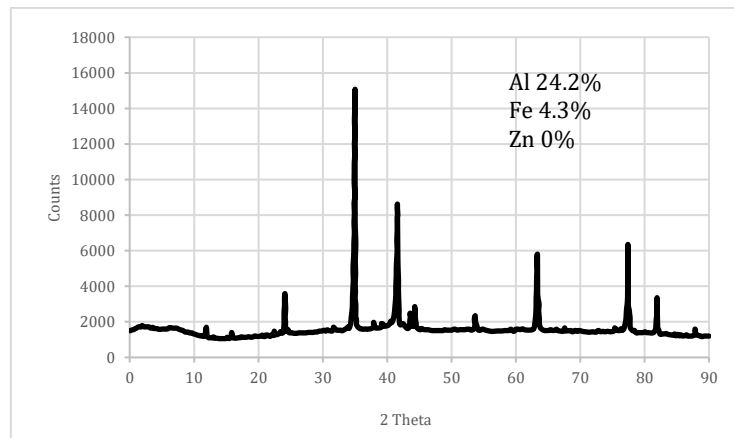
Fig. 7: XRD pattern of Al, Fe, Si, and Zn mechanical alloyed powders sintered at 700°C for 48h
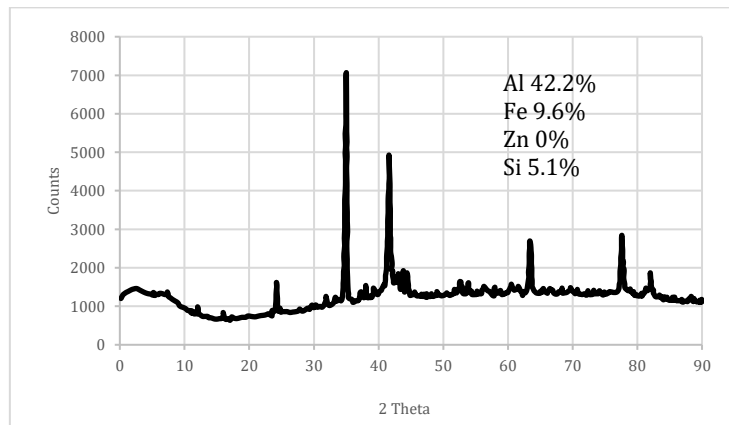
**Fig. 8:** XRD pattern of Al, Fe, Si, and Zn mechanical alloyed powders sintered at 700°C for 72h

Three distinct features which are classified as a matrix (dark gray), individual particles (light gray), and pores (bright area) are apparent in Fig. 9. This

supports the findings reported during XRD analysis that the second phase has formed in the Al, Fe, Si, Zn compacts. The matrix phase is a mixture of Al, Fe,

and Si which reacts with time at high temperature to form Fe-Al/AlFeSi intermetallic particles. This suggests that the reaction kinetics of Fe-based intermetallic formation is slow under given conditions which endorsed the findings of previous investigators (Carpenter et al., 2007).

Pores are an integral feature of particles fabricated via the powder metallurgy route. The brighter pores area is due to poor electron transfer which is most likely due to ZnO formed during the sintering process. This suggests oxygen presence in the vacuum furnace. The qualitative chemical composition of various points was determined via EDS analysis and is given in Table 2. The light gray phase is identified as AlFeSi intermetallic compound which was also reported during EDS analysis. Considering the slow reaction kinetics of solid phases, it has been demonstrated in this study that Fe-based intermetallic particles (AlFeSi) can be formed via a mechanical alloying route.
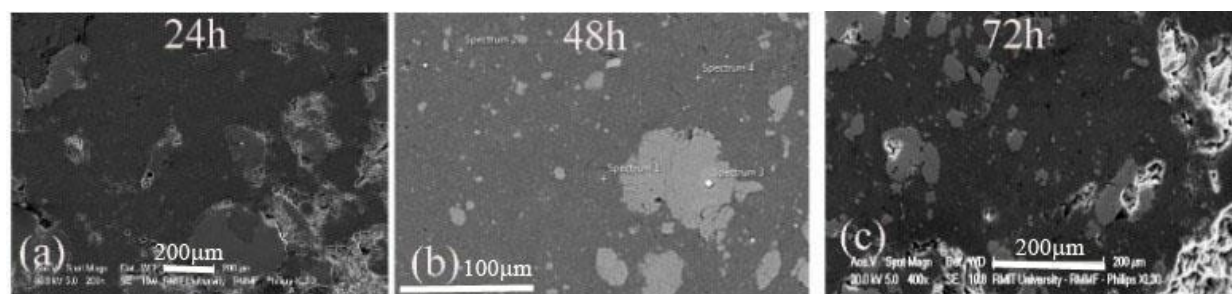

Fig. 9: SEM-SEI images of Al, Fe, Si, Zn compacts sintered at 700°C. (a) 24h, (b) 48h and (c) 72h

Table 2: EDS analysis of Al, Fe, Si, Zn compacts sintered at 700°C for 48h

Elements	EDS Points			
	1	2	3	4
Al	14.7	1.0	55.5	80.5
Fe	0.4	0.2	32.7	1.2
Si	84.3	98.3	10.0	13.3
Zn	0	0.2	Not detected	1.1
O	0.5	0.3	1.7	3.9

Zinc is volatilized during the sintering process even at 700°C hence not detected during EDS analysis as shown in Fig. 10. It is worth noting that Zn was added to fabricate T_{5c} Fe-based intermetallic particles which are the primary source of bottom dross in the galvanizing pots.

Al 55.5%
Fe 32.7%
O 1.7%
Si 10%
Zn 0.1%
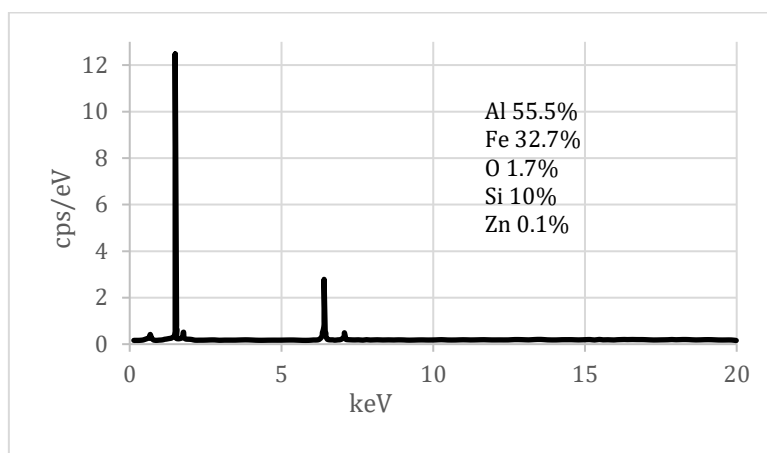
Fig. 10: EDS analysis of light gray phase in Fig. 9 (AlFeSi) at 48h

The chemical composition of AlFeSi intermetallic particles given in Fig. 10 is similar to that reported by earlier researchers (Peng et al., 2019). Zinc is the main difference between the chemical composition of bottom dross (AlFeSi(Zn)) and AlFeSi intermetallic particles.

4. Conclusion

In this study, the formation of Fe-based intermetallic (AlFeSi) via mechanical alloying is studied. It is concluded that:

- It is possible to produce Fe-based intermetallic particles through mechanical alloying and sintering processes.

- AlFeSi phase formed during mechanical alloying and its % increased from 38.9% to 55.5% which is an extraordinary observation.

- AlFeSi phase was observed during SEM analysis of the sintered compacts which endorsed the XRD findings.

- A maximum of 69% AlFeSi phase was recorded in the sintered compacts. The remaining Al, Fe, Si mechanically alloyed particles need further time to reach equilibrium and form Fe-Al/AlFeSi particles.

- Zinc volatilized during the sintering process therefore was not present in the AlFeSi intermetallic particles. Therefore, the chemical composition and crystal structure of the AlFeSi phase is different from that of bottom dross particles.

Acknowledgment

Compliance with ethical standards

Conflict of interest

The author(s) declared no potential conflicts of interest with respect to the research, authorship, and/or publication of this article.

References

Abro SH, Moria HA, Chandio A, and Al-Khazaal AZ (2020). Understanding the effect of Aluminium addition on forming the second phase particles on grain growth of micro-alloyed steel. Journal of Engineering, Technology and Applied Science Research, 10(1): 5153-5156. https://doi.org/10.48084/etasr.3243

Carpenter KR, Dippenaar R, Phelan D, and Wexler D (2007). Synthesis of intermetallics based on the fe-al-si-zn alloy system by magneto-mechanical milling of ductile elemental powders. Advanced Materials Research, 15: 1032-1037. https://doi.org/10.4028/www.scientific.net/AMR.15-17.1032

Chen RY and Yuen D (2012). Microstructure and crystallography of Zn-55Al-1.6 Si coating spangle on steel. Metallurgical and Materials Transactions A, 43(12): 4711-4723. https://doi.org/10.1007/s11661-012-1259-5

Elfghi MA and Gunay M (2020). Mechanical properties of powder metallurgy (Ti-6Al-4V) with hot isostatic pressing. Engineering, Technology and Applied Science Research, 10(3): 5637-5642. https://doi.org/10.48084/etasr.3522

Khaliq A, Parker DJ, Setargew N, and Qian M (2020). Fabrication of the τ 5c intermetallic compound monoliths by a novel powder metallurgy and hot-dipping approach. Metallurgical and Materials Transactions B, 51(2): 836-849. https://doi.org/10.1007/s11663-019-01765-z

Khaliq A, Parker DJ, Setargew N, Kondoh K, and Qian M (2021). Dissolution kinetics of iron-based intermetallic compounds (τ 5c IMCs) in a commercial steel strip metallic alloy coating process. Metallurgical and Materials Transactions B, 52(1): 41-50. https://doi.org/10.1007/s11663-020-01985-8

Luo Q, Jin F, Li Q, Zhang JY, and Chou KC (2013). The mechanism of dross formation during hot-dip Al-Zn alloy coating process. Journal for Manufacturing Science & Production, 13(1-2): 85-89. https://doi.org/10.1515/jmsp-2012-0023

Marder AR (2000). The metallurgy of zinc-coated steel. Progress in Materials Science, 45(3): 191-271. https://doi.org/10.1016/S0079-6425(98)00006-1

Masumoto H and Takebayashi H (1999). Bottom dross build-up in Al-Zinc coating bath. In the PacZAC 99, Kualalumpur, Malaysia.

Naeem K, Hussain A, and Abbas S (2019). A review of shaped charge variables for its optimum performance. Engineering, Technology and Applied Science Research, 9(6): 4917-4924. https://doi.org/10.48084/etasr.3153

Peng W, Wu G, Lu R, Lian Q, and Zhang J (2019). The evaluation on corrosion resistance and dross formation of Zn–23 wt% Al–0.3 wt% Si–x wt% Mg alloy. Coatings, 9(3): 199. https://doi.org/10.3390/coatings9030199

Selverian JH, Notis MR, and Marder AR (1987). The microstructure of 55 w/o Al-Zn-Si (Galvalume) hot dip coatings. Journal of Materials Engineering, 9(2): 133-140. https://doi.org/10.1007/BF02833702

Sheikhhasani H, Sabet H, and Abasi M (2016). Investigation of the effect of friction stir spot welding of BH galvanized steel plates on process parameters and weld mechanical properties. Engineering, Technology and Applied Science Research, 6(5): 1149-1154. https://doi.org/10.48084/etasr.678

Suryanarayana C (2001). Mechanical alloying and milling. Progress in Materials Science, 46(1-2): 1-184. https://doi.org/10.1016/S0079-6425(99)00010-9